Structural stability and magnetism of FeN from first principles

A. Houari,[1] S. F. Matar,[2,*] M. A. Belkhir,[1] and M. Nakhl[3]
[1]*Laboratoire de Physique Théorique, Departement de Physique, Université de Bejaia, 06000 Bejaia, Algeria*
[2]*Institut de Chimie de la Matière Condensée de Bordeaux, CNRS, Université Bordeaux 1, 33600 Pessac, France*
[3]*Faculté des Sciences et de Génie Informatique, Université St Esprit de Kaslik, Jounieh, Lebanon*
(Received 10 October 2006; revised manuscript received 30 November 2006; published 23 February 2007)

In the framework of density-functional theory, the structural and magnetic properties of FeN mononitride have been investigated using the all-electron augmented spherical wave method with a generalized gradient approximation functional for treating the effects of exchange and correlation. Calculation of the energy versus volume in hypothetic rocksalt (RS-), zinc-blende (ZB-), and wurtzite (W)-type structures shows that the RS-type structure is more stable than the others. Spin-polarized calculation results at equilibrium volume indicate that the ground state of RS-FeN is ferromagnetic with a high moment, while ZB-FeN and W-FeN are nonmagnetic. The influence of distortions on the stability is taken into account by considering FeN in two different face-centered-tetragonal structures (fcts): fct rocksalt and fct zinc blende. The magnetovolume effects with respect to Slater-Pauling-Friedel model are discussed. The electronic structures analyzed from site- and spin-projected density of states are reported. A discussion of the structural and magnetic properties of FeN is given with respect to N local environment of Fe.

DOI: 10.1103/PhysRevB.75.064420 PACS number(s): 72.25.Ba

I. INTRODUCTION

The study of the iron-nitrogen system has attracted much scientific importance for basic research as well as for technology. It was extensively investigated over two decades (1950–1970) following its first discovery by Jack.[1] A large number of results have been reported for Fe-rich nitrides (see Ref. 2 and references therein). This was motivated by their potential applications such as pigments for high-density magnetic recording.[3] On the contrary, only few reports are available in the case of the mononitride FeN,[4,5] which is considered as interesting material in the emergent spintronic field (sources of spin injection to semiconductors or diluted magnetic semiconductors). Recently, thin films of FeN have been synthesized and two possible crystal structures were reported.[6–9] One is the rocksalt (RS) structure with a lattice constant of $a=4.57$ Å, and by performing ^{57}Fe Mössbauer spectroscopy measurements, the authors suggested rocksalt FeN to be an antiferromagnet.[6,7] The other structure is of a zinc-blende (ZB)-type with a lattice constant of $a=4.33$ Å and a micromagnetic character.[8]

In order to achieve a better understanding of their physical properties and to discuss the experimental discrepancies, some theoretical investigations have been undertaken. From the available literature, a clear controversy exists between the studies carried out in the framework of density-functional theory. Shimizu *et al.*[10] have concluded that a ferromagnetic rocksalt FeN is more stable than nonmagnetic zinc-blende nitride. The same results were reported later on the stability of the FeN RS-type structure, but without complete agreement for the magnetic ordering.[11,12] However, Lukashev and Lambrecht[13] have joined some others[14] in predicting a stable nonmagnetic ZB structure for FeN. In this context and in order to provide an improved theoretical explanation, we carried out comprehensive spin-density-functional calculations in both ZB and RS phases. Further, for a better investigation of the magnetic properties with respect to the structural aspects, we have also considered FeN in the hexagonal wurtzite-type structure. With the sophisticated techniques of synthesis reached recently (synthesis of thin films and nanowires, etc.), the structural distortions may have important effects on the investigated physical properties. To take into account the effects of some possible distortions, we have also investigated FeN in the face-centered-tetragonal (fct) structure. As a matter of fact, the manganese mononitride (MnN) has been recently found in (fct-RS)-type structure, i.e., a tetragonally distorted rocksalt structure.[15] In our case, we have considered FeN in both tetragonally distorted rocksalt structure (fct-RS) and tetragonally distorted zinc-blende (fct-ZB) structure for the sake of completeness. The structural, electronic, and magnetic properties are thus reviewed by analyzing the calculated electronic structure, total energies, and crystal-field influence. A description of the computational details is given in Sec. II. Our results for the calculated total energy and magnetic moment are presented in Sec. III, with a discussion of the magnetovolume effects. Section IV is devoted to the Slater-Pauling-Friedel model as applied to iron nitrides. In Sec. V, the nonmagnetic results are discussed in the framework of the Stoner theory of band ferromagnetism. Section VI details the electronic structure via partial density of states analysis. Finally, a conclusion and a prospective for future developments are given in the last section.

II. COMPUTATIONAL DETAILS

Our first-principles calculations are performed in the framework of the density-functional theory[16,17] using the generalized gradient approximation (GGA) with the Perdew-Burke-Ernzerhof (PBE) parametrization for the exchange and correlation.[18] This parametrization scheme was preferred over the local-density approximation (LDA) in view of the results on iron nitrides cited in this work.[10,12] Self-consistent calculations were carried out using the scalar-relativistic augmented spherical wave (ASW) method[19,20] based on the

atomic sphere approximation (ASA). In this method, the value of the GGA-PBE *kappa* was fixed to 0.8. In the ASW method, the wave function is expanded in atom-centered augmented spherical waves, which are Hankel functions and numerical solutions of Schrödinger's equation, respectively, outside and inside the so-called augmentation spheres. In order to optimize the basis set, additional augmented spherical waves were placed at carefully selected interstitial sites. The choice of these sites as well as the augmentation radii were automatically determined using the sphere-geometry optimization algorithm.[21] The basis set consisted of Fe$(4s,4p,3d)$ and N$(2s,2p)$ valence states. The Brillouin-zone integrations were performed with an increasing number of k points $(16\times16\times16)$ in order to ensure convergence of the results with respect to the k-space grid. The convergence criterion is fixed to 0.001 mRy in the self-consistent procedure and charge difference $\Delta Q=10^{-4}$ between two successive iterations. In order to establish a reference for the spin-polarized calculations, we started with a set of spin-degenerate calculations. We note that this does not represent a paramagnetic situation which would require heavy computations involving large supercells with random spin orientations. It allows assigning a role to the orbitals responsible of the magnetic instability toward spin polarization in a mean-field analysis using the Stoner theory of band ferromagnetism.[22]

III. RESULTS FOR THE TOTAL ENERGY AND THE MAGNETIC MOMENTS

In a collective electron scheme, such as the one used here, the magnetization arises from interband spin polarization; i.e., it is mediated by the electron gas. This is opposite to the localized electron moments where magnetization arises from intraband spin polarization such as in oxide systems, especially insulating ones. From this, it is expected that the magnetovolume effects will be large in intermetallic and insertion alloy systems. The theoretical equilibrium volume and the structural preference of the FeN compound are obtained by calculating the variation of the total energy versus the volume of the cubic cell in the rocksalt and zinc-blende structures. For wurtzite, fct rocksalt, and fct zinc blende, the same procedure (total energy versus the volume of the unit cell) was done twice, in order to obtain the two equilibrium lattice constants a and c which determine the equilibrium volume. The stability toward magnetism in each phase is given by comparing the spin-polarized (SP) and the non-spin-polarized (NSP) total-energy values at theoretical equilibrium volume. With the same k-point grids of the reciprocal lattice and for different pairs (E,V), after a fitting with a Birch equation of state,[25] we obtain after convergence a quadratic curve with a minimum (E_0,V_0). Figures 1(a) and 1(b) show the energy versus volume curves of FeN in the RS and ZB structures for NSP and SP cases, respectively. For the wurtzite structure, Fig. 1(c) shows the energy variation versus volume at the equilibrium c lattice constant, i.e., the variation of energy versus the a lattice constant. Because the fct-rocksalt and fct-zinc-blende structures are derived from the cubic ones, the same variation is observed and the results are not plotted here. The results for theoretical lattice constants, total energy, and other equilibrium properties are summarized in Table I for all the studied structures with the experimental data for the lattice constants.

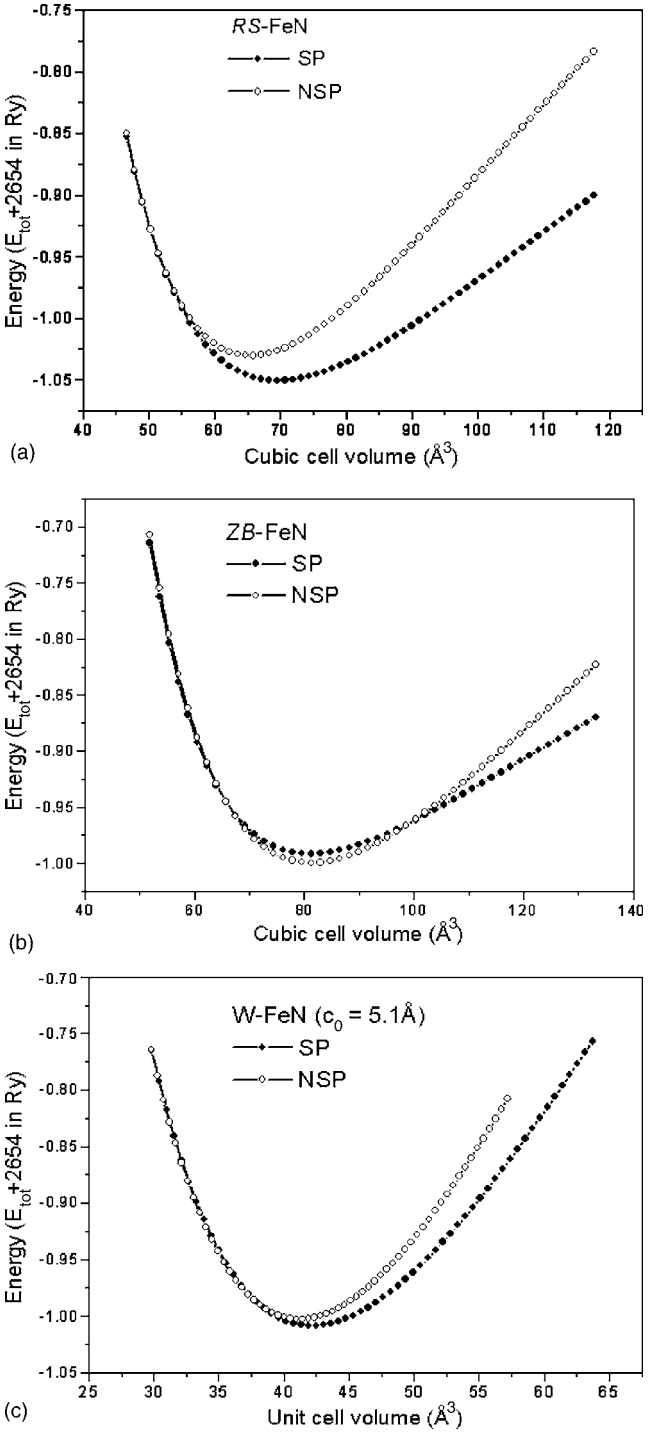

FIG. 1. Spin-polarized (SP) and non-spin-polarized (NSP) total energy versus volume in (a) RS-FeN, (b) ZB-FeN, and (c) W-FeN at equilibrium c_0 lattice constant for the latter.

Figure 1(a) shows that the ferromagnetic state of FeN in the RS phase is preferred at the calculated equilibrium volume to the nonmagnetic state. On the contrary, the magnetic order in ZB and W phases can be favored but only at higher volume [see Figs. 1(b) and 1(c)]. At equilibrium, the energy

TABLE I. Calculated equilibrium properties [in atomic units (bohrs) 1 Ry=13.6 eV] for FeN nitride in five different structures: rocksalt (RS), zinc-blende (ZB), wurtzite (W), face-centered-tetragonal-rocksalt (fct-RS), and face-centered-tetragonal-zinc-blende (fct-ZB).

Equilibrium properties	Lattice constants (Å)	Total energy (Ry)	$d_{\text{Fe-N}}$ (Å)	m_{tot} (μ_B)
NSP-RS	a=4.026	−2655.026	2.004	
SP-RS	a=4.11	−2655.047	2.004	2.60
	a=3.999[a]			
	a=4.20[b]			
	Expt: a=4.571[c]			
AF-RS		−2655.046	2.058	2.36
NSP-ZB	a=4.338	−2654.997	1.870	
SP-ZB	a=4.348	−2654.998	1.879	0.00
	a=4.359[a]			
	a=4.197[d]			
	Expt: a=4.332[e]			
NSP-W	a=3.057	−2655.018	1.908	
	c=5.098			
SP-W	a=3.073	−2655.019	1.909	0.00
	c=5.098			
NSP-fct-RS	a=4.12	−2655.022	2.047	
	c=4.01			
SP-fct-RS	a=4.15	−2655.044	2.076	2.63
	c=4.05			
AF-fct-RS		−2655.045	2.076	2.48
NSP-fct-ZB	a=4.28	−2654.992	1.864	
	c=4.24			
SP-fct-ZB	a=4.30	−2654.993	3.525	0.00
	c=4.24			

[a]Reference 10.
[b]Reference 12.
[c]Reference 6.
[d]Reference 13.
[e]Reference 8.

difference between the ferromagnetic and nonmagnetic states in these two structures are nearly zero, thus instability toward magnetism could exist. This instability may be the reason of the micromagnetic character observed experimentally for FeN in ZB structure. From Table I, our estimated theoretical lattice constant in the SP case (a=4.348 Å) agrees well with the experimental data for the ZB phase. However, a large difference exists between the obtained theoretical lattice constant (a=4.11 Å) and the experimental reports (a_{expt}=4.57 Å) in the RS structure. It is important to mention that our results for this point are in good agreement with all the theoretical studies of the FeN reported in the literature (even those predicting a ZB stable structure for FeN), but surprisingly, up to now, no one was able to reproduce the experimental data.

The common explanation put forward to explain this large difference is that it would originate firstly from surface effects because the samples were grown as thin films, and secondly from the nonstoichiometry of the elaborated samples. The values of the total energies in Table I indicate that the FeN compound in the ferromagnetic state should be more stable in RS structure than in ZB or W ones. At equilibrium, FeN in these two latter structures has a zero magnetic moment, while the unit cell of RS-FeN possesses a moment of $2.62\mu_B$ (a moment of $2.51\mu_B$ per Fe atom). Our results are in good agreement with those reported by Shimizu *et al.*[10] concerning the ferromagnetic order of FeN. A value of $2.67\mu_B$ was reported by Kong but in a stable antiferromagnetic (AFM) RS-FeN.[12].

We also performed antiferromagnetic (AF) calculations at the ferromagnetic equilibrium lattice constant in order to check for a possible instability toward such a magnetic configuration for the ground state, as suggested by Nagakawa *et al.*[6] and Hinomura and Nasu.[7] Among possible spin arrangements, we examined for this purpose the [001] alignment (AF [001]) in which the spins are parallel within a layer but alternating direction between adjacent layers in the [001] direction. From carefully converged calculations, the results in Table I indicate that the energies of AF and ferromagnetic (FM) states for FeN in RS structure remain very close. Moreover, in fct-rocksalt structure, the former one seems more stable. The energy differences between AF and FM states are too small to make a clear conclusion on the nature of the magnetic order in the two crystal varieties. On the other hand, the energy difference between RS-FeN and fct-RS-FeN is very small, thus one can believe that under some elaboration conditions, FeN nitride can crystallize in a face-centered- tetragonal-rocksalt structure. Because of this, the AF character observed experimentally can be explained either by this AF-FM instability in the RS-structure or by some lattice distortions which stabilize the FeN compound in AF-fct-rocksalt structure.

In earlier investigations[26] on the magnetovolume effects in the Fe_4N nitride, it has been shown that there is a transition from "low moment–low volume" to "high moment–large volume" which resembles the moment versus volume dependence of γFe. This behavior seems to occur in all structures studied here of equiatomic FeN nitride. As can be seen in Fig. 2, the variation of the moment in RS-FeN (and in fct-RS-FeN which is not shown here) is very similar to those of Fe II (located at the faces of the cubic cell) in Fe_4N. In ZB-FeN (and in fct-ZB-FeN also not shown here), a sudden increase from zero to a value as high as $2.85\mu_B$ occurs at high volume, such as the behavior of Fe I atoms (located in the corners) in Fe_4N. The same variation of the magnetic moment is indicated for W-FeN.

An analysis of the effects of the Fe-N spacing on the magnetic moment value shows that the Fe-N distances, corresponding to equilibrium of zinc-blende, fct-zinc-blende, and wurtzite structures (see Table I), give a nonzero moment (around $1\mu_B$) in rocksalt and/or fct-rocksalt structure. If we consider the similar increase of the magnetic moment value reported elsewhere in CsCl-type FeN,[12] one should recognize that at different atomic environments (crystalline structures) even with the same Fe-N distance, different values of the

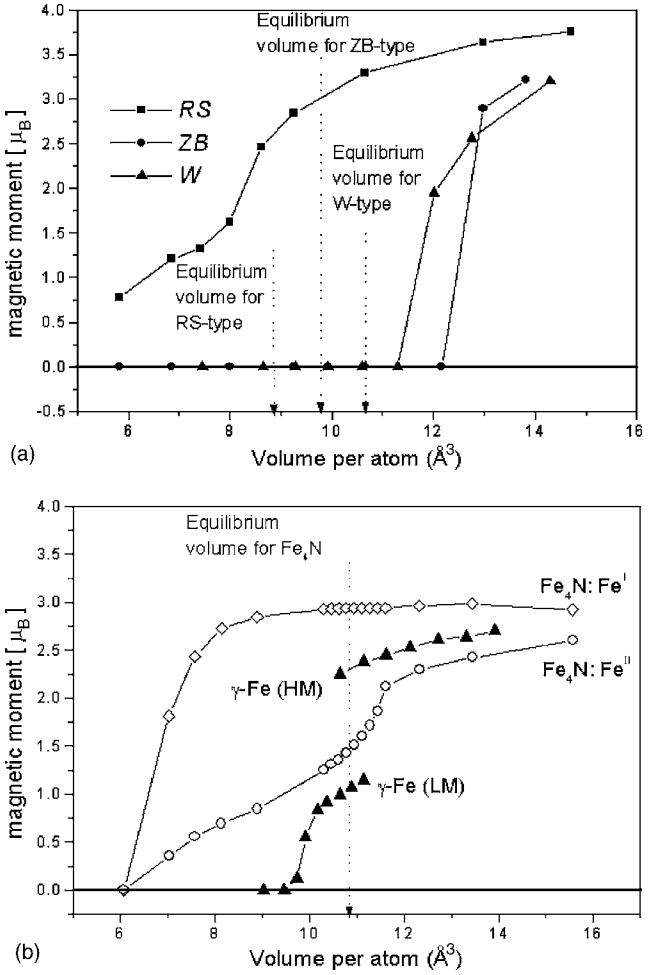

FIG. 2. Magnetic moment versus volume in (a) present work: FeN in RS, ZB, and W structures. (b) Fe_4N and γ Fe (replotted from Ref. 26).

moment are obtained. Thus, the major effect which prevails in the value of the magnetic moment is the nature of the *d-p* hybridization in the Fe–N bond which is related to the atomic environment (the number of the nearest neighbors), and the Fe-N distance has only an average effect.

IV. ANALYSIS WITHIN THE SLATER-PAULING-FRIEDEL MODEL

The magnetic moment variation with valence electron count can be discussed by means of the Slater-Pauling model.[22] This is mainly illustrated by the Slater-Pauling curve which is a plot of the average magnetic moment μ_{av} with the valence electron count Z_v for intermetallic alloy systems characterized by strong ferromagnetism. From the plot, the variation of the average magnetization of an alloy with the solute concentration can be obtained. For most of the magnetic systems, either the majority ($\uparrow$) or minority ($\downarrow$) spin population is known. The magnetization being provided by the difference of electron occupation between the majority ($\uparrow$) and the minority ($\downarrow$) spins, the following relationships can be established: $m=n(\uparrow)-n(\downarrow)$ and $Z_v=n(\uparrow)+n(\downarrow)$.

TABLE II. Application of the Slater-Pauling-Friedel model of the magnetic valence to iron nitrides (see text).

Iron nitride	Z_v	Z_m	m_{SPF} (μ_B) $=Z_m+0.6$	m_{ASW} (μ_B)
Fe_8N[a]	7.44	1.44	2.04	2.17
Fe_4N[a]	7.0	1.0	1.60	1.67
Fe_3N[a]	6.75	0.75	1.35	1.44
Fe_2N[a]	6.33	0.33	0.93	0.95
FeN (from Fe_2N)[a]	5.5	−0.5	0.10	0.00
FeN	5.5	−0.5	0.10	0.00 (ZB)
				0.00 (W)
				2.62 (RS)
				2.60 (fct-RS)
				0.00 (fct-ZB)

[a]Reference 27.

Hence, m, the magnetic moment, can be obtained either as $m=2n(\uparrow)-Z_v$, if $n(\uparrow)$ is known, or $m=Z_v-2n(\downarrow)$, if $n(\downarrow)$ is known. These two expressions for m describe two branches with opposite 45° slopes of the Slater-Pauling curve around which the experimental points are gathered. If one assumes that the magnetic moment mostly arises from *d*-band polarization, the quantity "magnetic valence" can be defined here for systems where $n_{d(\uparrow)}$ is known as $Z_m=2n_{d(\uparrow)}-Z_v$. Upon alloying, the electron count of the *d* states changes in a discrete way, as treated by Friedel,[24] so that $n_{d(\uparrow)}$ is either 0 (early transition elements) or 5 (late transition elements). For instance, for Fe, Z_v is 8 and $Z_m=10-8=2$, whereas for N ($n_{d(\uparrow)}=0$), $Z_v=3$ and $Z_m=0-3=-3$. This leads to an alternative representation called Slater-Pauling-Friedel (SPF) curve where μ_{av} is plotted against Z_m: $\mu_{av}=Z_m+0.6$. In this writing, the figure 0.6 is a nearly constant contribution to the magnetic moment arising from *s* and *p* electrons. The calculated atom-averaged magnetic moments (μ_{av}) via the expression above and from ASW calculations are summarized in Table II. The results of the present study (for FeN nitride) are shown in the last line of the table; the other data are from Ref. 27 in which the SPF model was applied for the whole series of the Fe-N systems. In their study, Matar and Mohn[27] have found good agreement between SPF model and ASW calculation results, and all average moments decrease with increasing amount of nitrogen. While our obtained moments in ZB-FeN, fct-ZB-FeN, and W-FeN agree well with SPF model in finding a vanishingly small magnetization, a large discrepancy exists in the case of RS-FeN and fct-RS-FeN which carry large magnetizations. This interestingly points to the limits of the SPF model which is an average scheme dealing with the electronic configuration of the chemical species present, and does not account for the nature of the crystalline structure and the chemical bonding.

V. MEAN-FIELD ANALYSIS OF NONMAGNETIC CONFIGURATIONS

Within the Stoner theory of band ferromagnetism,[23] which is a mean-field approach, the large density of states (DOS) at

the Fermi level $n(E_F)$ is related to the instability of the nonmagnetic state with respect to the onset of intraband spin polarization. When $n(E_F)I_s > 1$ where I_s is the Stoner integral, calculated and tabulated by Janak[28] for the elemental systems, then the nonmagnetic state is unstable with respect to the onset of magnetization. In the RS-FeN type with a density of states at the Fermi level $n(E_F)=71.596$ states/(Ry Fe) and a Stoner parameter $I_s=0.034$ Ry, the Stoner criterion is fulfilled (2.434). On the contrary, for the ZB-FeN and W-FeN, we have $n(E_F)=14.106$ states/(Ry Fe) and $n(E_F)=15.152$ states/(Ry Fe), respectively; the Stoner criterion (0.48 and 0.515) is not fulfilled. As a consequence, the magnetic behavior of FeN is consistent with the Stoner theory. As discussed in the literature, the magnetic moment of Fe atom in FeN (Refs. 10, 12, and 13) and generally in the Fe nitrides[2] is very sensitive to the nearest-neighboring Fe-N distance and their *d-p* hybridization. Our results confirm that this latter is the most important effect.

VI. DENSITY OF STATES IN THE FERROMAGNETIC CONFIGURATION

Considering the results obtained for the electronic structure of FeN at equilibrium, we discuss the electronic structure from the plots of the DOS. Spin polarization results from a nearly rigid band shift between the majority spins (↑) to lower energy and minority spin (↓) to higher energy due to the gain of energy from exchange. The site- and spin-projected partial DOS (PDOS) are shown in Fig. 3 for RS-FeN and ZB-FeN at the theoretical equilibrium lattice constants. The W-FeN PDOSs which resemble those of ZB-FeN are not presented here. Energy low-lying N(2*s*) states at ~ -10 eV as well as ES(PDOS) of vanishingly low intensity are not shown. As a matter of fact, ESs receive charge residues from actual atomic spheres and they are known to ensure covalency effects in such systems.[2] Note that in RS-FeN, the octahedral environment splits the Fe 3*d* states into t_{2g} and e_g manifolds, whereas in the tetrahedral environment of ZB-FeN, the *d* states are split into *e* and t_2 manifolds. These respective environments result in totally different DOS features within the two structures: whereas they are continuous over the VB in RS-FeN, more localization is observed for the ZB-FeN. One consequence is that RS-FeN is a metal through the itinerant e_g states crossing the Fermi level, while in ZB-FeN the system is close to an opening of gap at E_F. Within the valence band (VB), two parts can be considered. While the lower energy part, centered at −5 eV, is mainly composed of N 2*p* states mixing with itinerant Fe-e_g ones, the higher-energy part from −3 to 1 eV is dominated by the Fe-t_{2g} states which are localized and thus responsible of the magnetic moment (RS-FeN). These states are moved to lower energy for (↑) spin population (upper panel) and hence are found below the Fermi level E_F, whereas for the minority-spin (↓) the DOS peaks are located above E_F (lower DOS half panel). This is due to the exchange splitting, whose absence in the ZB-FeN PDOS causes mirror PDOS in upper and lower half panels of Fig. 3(b). Clearly, the T_d crystal field is unfavorable to the onset of magnetization in ZB-FeN and *a fortiori* in W-FeN.

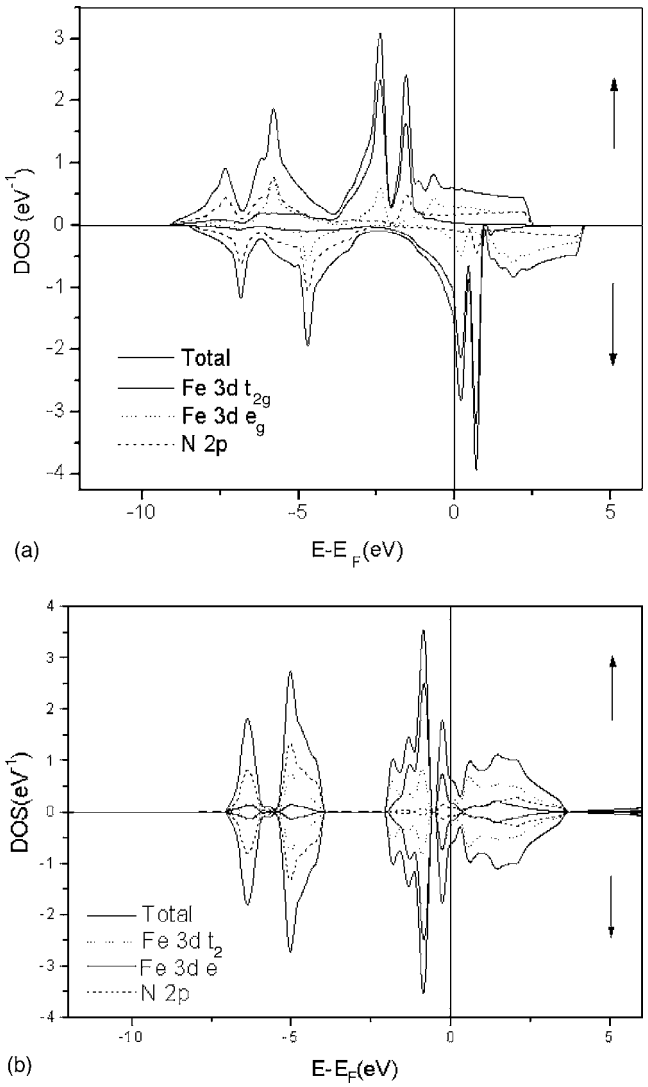

FIG. 3. Spin-polarized total and partial density of states (PDOS) of (a) RS-FeN and (b) ZB-FeN at equilibrium lattice constants in the ferromagnetic state.

VII. CONCLUSION

With the use of the self-consistent DFT-based ASW method, we have investigated the structural, electronic, and magnetic properties of the iron mononitride (FeN) in the rocksalt (RS), zinc-blende (ZB), and wurtzite (W) structures. We have also investigated the effects of distortion by considering FeN in a tetragonally distorted rocksalt fct-RS and in a tetragonally distorted zinc-blende fct-ZB structures. The calculated total energy shows that FeN is stabilized in a ferromagnetic (FM)-rocksalt structure with a theoretical lattice constant $a=4.11$ Å and a magnetic moment of $2.62\mu_B$. While ZB-FeN and W-FeN types seem to prefer a paramagnetic order at theoretical equilibrium, they possess nevertheless a nonzero magnetic moment at higher lattice constant. This involves strong magnetovolume effects which are equally accompanied by crystal field ones, depending on whether the local environment is octahedral or tetrahedral. The equilibrium energies of nonmagnetic and FM states of

ZB-FeN are very close and this instability toward magnetism may be the reason for the micromagnetic character observed experimentally. We have also found a very small energy difference between RS-FeN and fct-RS-FeN; thus, one can predict that in some special synthesis conditions such as the presence of strains in the growth of layers of iron mononitride, FeN could crystallize in the latter structure. The energies of AF and FM states in RS-FeN and fct-RS-FeN are too close, so it is difficult to make a clear conclusion on the nature of the magnetic order of the ground state for these structures. As suggested in the literature, the present work confirms that the magnetic properties of FeN are dominated by *p-d* hybridization of the Fe-N interaction. However, we have found that the Fe-N distance has only an average effect on the value of the magnetic moment. On the other hand, our results of FeN compound complete the finding on the competition between chemical and magnetovolume effects in the series of iron nitrides: Fe_8N, Fe_4N, and Fe_3N as well as Fe_2N.[29] For FeN in ZB- and W-type structures, good agreement with Slater-Pauling-Friedel model, connecting average magnetization with valence, is found; but when RS-FeN is considered, a large difference exists so that other effects related with the nitrogen environment of Fe (O_h versus T_d or C_{4v}) should become prevailing. As a prospective, we think of completing the explanation of the FeN properties in two complementary directions: by considering slab and surface calculations and by taking into account non- (i.e., sub- or super-) stoichiometries in extended lattices. (This should comply with the nature of the samples elaborated experimentally which point to N substoichiometric FeN_{1-x} compositions.) Such investigations will call for heavy calculations involving other computational frameworks such as the use of pseudopotential based codes for geometry optimizations.[30] The studies are underway.

ACKNOWLEDGMENTS

One of the authors (S.F.M.), acknowledges computational facilities provided by the M3PEC-Regional Mesocenter of the University Bordeaux 1 (http://www.m3pec.u-bordeaux1.fr). Discussions at an early stage of this work with Professor Dr. Peter Mohn of the University of Vienna, Austria, are equally acknowledged.

*Corresponding author. Electronic address: s.matar@u-bordeaux1.fr

[1] K. Jack, Proc. R. Soc. London, Ser. A **11**, 34 (1948).
[2] S. F. Matar, J. Alloys Compd. **345**, 72 (2002).
[3] S. F. Matar, G. Demazeau, and B. Siberchicot, IEEE Trans. Magn. **26**, 60 (1990).
[4] N. Heinman and N. S. Kazama, J. Appl. Phys. **52**, 3562 (1981).
[5] A. Oueldennaoua, E. Bauer-Grosse, M. Foos, and C. Frants, Scr. Metall. **19**, 1503 (1985).
[6] H. Nakagawa, S. Nasu, M. Takahashi, and F. Kanamaru, Hyperfine Interact. **69**, 455 (1991).
[7] T. Hinomura and S. Nasu, Hyperfine Interact. **111**, 221 (1998).
[8] K. Suzuki, H. Morita, T. Kaneko, H. Yoshida, and H. Fujimori, J. Alloys Compd. **201**, 11 (1993).
[9] L. Rissanen, M. Neubauer, F. P. Lieb, and P. Schaaf, J. Alloys Compd. **274**, 74 (1998).
[10] H. Shimizu, M. Shirai, and N. Zuzuki, J. Phys. Soc. Jpn. **67**, 922 (1998).
[11] A. Filippetti and W. E. Pickett, Phys. Rev. B **59**, 8397 (1999).
[12] Y. Kong, J. Phys.: Condens. Matter **12**, 4161 (2000).
[13] P. Lukashev and Walter R. L. Lambrecht, Phys. Rev. B **70**, 245205 (2004).
[14] B. Eck, R. Dronskowski, M. Takahashi, and S. Kikkawa, J. Mater. Chem. **9**, 1527 (1999).
[15] K. Suzuki, Y. Yamaguchi, T. Kaneko, H. Yoshida, Y. Obi, H. Fujimori, and H. Morita, J. Phys. Soc. Jpn. **201**, 1084 (2001).
[16] P. Honenberg and W. Kohn, Phys. Rev. **136**, B864 (1964).
[17] W. Kohn and L. J. Sham, Phys. Rev. **140**, A1133 (1965).
[18] J. P. Perdew, K. Burke, and M. Ernzerhof, Phys. Rev. Lett. **77**, 3865 (1996).
[19] A. R. Williams, J. Kübler, and C. D. Gelatt, Phys. Rev. B **19**, 6094 (1979).
[20] V. Eyert, Int. J. Quantum Chem. **77**, 1007 (2000).
[21] V. Eyert and K.-H. Höck, Phys. Rev. B **57**, 12727 (1998).
[22] J. Kübler and V. Eyert, in *Electronic and Magnetic Properties of Metal and Ceramics* edited by K. H. J. Buschow (VCH Verlaggesellschaft, Weinheim, 1991).
[23] D. M. Roy and D. G. Pettifor, J. Phys. F: Met. Phys. **7**, L183 (1977).
[24] J. Friedel, Nuovo Cimento **10**, 287 (1958).
[25] G. Birch, J. Geophys. Res. **83**, 1257 (1978).
[26] P. Mohn and S. F. Matar, J. Magn. Magn. Mater. **191**, 234 (1999).
[27] S. F. Matar and P. Mohn, Active and Passive Electron. Components **15**, 89 (1993).
[28] J. F. Janak, Phys. Rev. B **16**, 255 (1977).
[29] S. F. Matar, C. R. Chim. **5**, 539 (2002).
[30] VASP code, G. Kresse and J. Hafner, Phys. Rev. B **47**, 558 (1993); G. Kresse and J. Furthmüller, Comput. Mater. Sci. **6**, 15 (1996).